Characterization of a Current-Mode Bandgap Circuit Structure for High-Precision Reference Applications

Hanqing Xing, Le Jin, Degang Chen, and Randall Geiger
Department of Electrical and Computer Engineering
Iowa State University
Ames, IA 50011, USA
xinghq@iastate.edu, ljin@iastate.edu, djchen@iastate.edu, rlgeiger@iastate.edu

***Abstract*— In this paper, the well-known equation, which explicitly shows the temperature behavior of the I_C-V_{BE} characteristics of the transistor, is applied to analyze a specific bandgap reference circuit. The theoretical analysis clearly characterizes some important features of the circuit, such as the value of the bandgap output, the relationship of the inflection point and the circuit parameters, the curvature of the bandgap curve and so on. Spectre simulations show a good consistency of the analysis. Based on the analysis, a new approach for designing high-precision references is also proposed.**

I. INTRODUCTION

References such as voltage references and current references are widely used in electronic systems that support both the consumer market and the defense industry. The thermal stability of the references plays a key role in the performance of many of these systems. Most of the bandgap reference circuits utilize the linear combination of the base-emitter voltage (V_{BE}) and the thermal voltage (kT/q), whose temperature coefficients (TC) are opposite in sign, to generate references. Therefore, although the individual outputs have rather high temperature coefficients, the temperature sensitivity of the bandgap reference is reduced considerably [1]. However, the thermal voltage can only compensate the first-order negative temperature dependence of V_{BE}. The nonlinear temperature dependence of the base-emitter voltage still remains and dominates the performance of the bandgap reference [2] [3]. Those bandgap references with linear compensation normally have a parabolic temperature dependence curve near the inflection point. Those references are capable of achieving temperature coefficients ranging from 20ppm/°C to 100ppm/°C over 100°C. To achieve higher precision voltage reference, different techniques, such as nonlinear correction and curvature compensation technique, have been developed to cancel the nonlinear temperature dependent components in addition to the linear term [4]. By applying nonlinear compensation, the temperature coefficients under 10ppm/°C can be obtained over a 100°C range. The details of recent advanced low TC CMOS bandgap voltage reference can be found in [4]

Unfortunately, most of emerging systems depend upon 14-bit and 16-bit data converters. If a whole least significant bit variation in the reference voltage over temperature could be tolerated, the temperature coefficient of a reference that operates over 100°C temperature range would need to be ±0.076ppm/°C for 16-bit systems, ±0.31ppm/°C for 14-bit systems, and ±1.22ppm/°C for 12-bit systems. As a result, the best references available from industry no longer meet the performance requirements of those systems.

In this work, through the explicit analysis of the thermal behavior of the specific bandgap circuit, its characteristics are systematically investigated. A new approach for designing high-precision references is proposed based on the analysis. The rest of the paper is organized as follows. Section 2 describes the bandgap circuit structure and theoretically analyzes the thermal characteristics of the circuit; Section 3 discusses the proposed method and Section 4 concludes the paper.

II. ANALYSIS AND CHARACTERIZATION OF BANDGAP STRUCTURE

In this section, a current mode bandgap structure will be described, and then some basic characteristics of the circuit are theoretically analyzed.

A. Description of the Low-voltage Bandgap Structure

Fig. 1 shows the bandgap circuit proposed by Banda [5], which is composed of a CMOS op-amp, two diode-connected bipolar transistors, CMOS transistors forming a current mirror

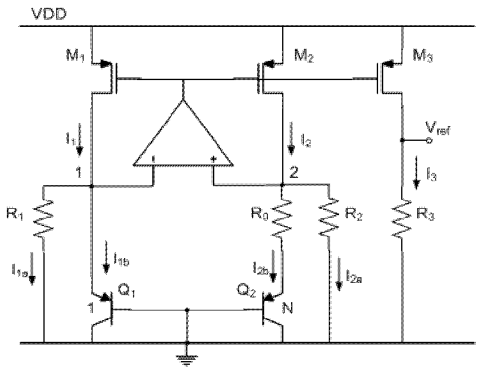

Figure 1. Schematic of the bandgap Circuit

This work is supported by the National Science Foundation.

and resistors. Assume the op-amp in the circuit is ideal with infinite DC gain and zero offset voltage. M_1, M_2 and M_3 are matched. R_1 equals R_2. Therefore, node voltages V_1 and V_2 are equal, current I_1 is equal to current I_2, and I_{1a} =I_{2a}, I_{1b} =I_{2b}. Two types of currents, I_{1a} (I_{2a}) and I_{2b} (I_{1b}), are generated in the circuit. I_{1a} (I_{2a}) is a current proportional to V_{BE} of Q1 and has a negative temperature coefficient. For I_{2b} (I_{1b}), it is a PTAT current generated by R_0 and ΔV_{BE} of Q_1 and Q_2. By an appropriate R_1/R_0 ratio and N, the linear compensation of the temperature dependence of the current I_1 (I_2) can be achieved. A bandgap voltage reference is formed by passing this bandgap current through a resistor R3. The magnitude of V_{ref} can be adjusted for different application by a proper R_3.

B. Theoretical Analysis of theBandgap Circuit

The analysis is based on the same assumptions above. Thus, we have V_1=V_2 and I_1=I_2. The two relationships can be expressed as

$$\frac{V_1}{R_1} + I_{1b} = \frac{V_1}{R_2} + I_{2b}, \tag{1}$$

and

$$|V_{BE1}| = |V_{BE2}| + I_{2b}R_0, \tag{2}$$

where V_{BE1} and V_{BE2} represent the base-emitter voltages of Q_1 and Q_2 respectively, and the currents are defined in Fig. 1. The currents through Q_1 and Q_2 can be written as

$$I_{1b} = \sigma A_1 T^r \exp(\frac{|V_{BE1}| - V_G}{kT/q}), \tag{3}$$

and

$$I_{2b} = \sigma A_2 T^r \exp(\frac{|V_{BE2}| - V_G}{kT/q}), \tag{4}$$

where σ is a temperature-independent constant, A_1 and A_2 are the base-emitter junction areas of Q_1 and Q_2, T is the temperature in K, r is also temperature-independent and depends on the doping level in the base, k is Boltzman's constant, q is the charge of an electron, and V_G is the bandgap voltage of silicon [1]. V_G can be further expressed as

$$V_G = V_{G0} - \frac{\alpha T^2}{T+\beta}. \tag{5}$$

For the silicon the values for the constants in (5) are, α=$7.021\times10^{-4}V/K$ and β=$1108K$ [2]. $V_G(0)$ is given as $1.17V$ in [2]. Since R_1=R_2, from (1) we know I_{1b}=I_{2b}. From (3) and (4), we can solve for

$$|V_{BE2}| = |V_{BE1}| + \frac{kT}{q}\ln\frac{A_1}{A_2}. \tag{6}$$

Substituting (6) back into equation (2), we get the expression

$$|V_{BE1}| = \frac{kT}{q}\ln(\frac{k}{qR_0\sigma A_1 T^r}\ln\frac{A_2}{A_1}) + V_G, \tag{7}$$

and consequently

$$I_{1b} = I_{2b} = \frac{kT}{qR_0}\ln\frac{A_2}{A_1}. \tag{8}$$

Then the current I_1 and I_2 can be derived as

$$\begin{aligned} I_1 &= I_2 \\ &= I_{1b} + \frac{|V_{BE1}|}{R_1} \\ &= \frac{kT}{qR_0}\ln\frac{A_2}{A_1} + \frac{kT}{qR_1}\ln(\frac{k}{qR_0\sigma A_1 T^{r-1}}\ln\frac{A_2}{A_1}) + \frac{V_G}{R_1} \end{aligned}. \tag{9}$$

Then the voltage reference is given by

$$\begin{aligned} V_{ref} &= I_3R_3 \\ &= I_1R_3 \\ &= \frac{R_3}{R_0}\frac{kT}{q}\ln\frac{A_2}{A_1} + \frac{R_3}{R_1}[\frac{kT}{q}\ln(\frac{k}{qR_0\sigma A_1 T^{r-1}}\ln\frac{A_2}{A_1}) + V_G] \end{aligned}. \tag{10}$$

It is noted that the temperature coefficient of the resistors, which is assumed the same for all the resistors, is cancelled by the resistance ratio in (10). So they are neglected in the following analysis. Then the thermal characteristics of V_{ref} are the same as those of the current I_1. Based on the analysis above, we can talk about the characteristics of the circuit.

1) The inflection point temperature

From (9), the partial derivative of I_1 with respect to the temperature is

$$\begin{aligned} \frac{\partial I_1}{\partial T} = &\frac{k}{qR_0}\ln\frac{A_2}{A_1} + \frac{k}{qR_1}\ln(\frac{k}{qR_0\sigma A_1 T^{r-1}}\ln\frac{A_2}{A_1}), \\ &-\frac{k(r-1)}{qR_1} - \frac{2\alpha T}{(T+\beta)R_1} + \frac{\alpha T^2}{(T+\beta)^2 R_1} \end{aligned} \tag{11}$$

where the temperature dependence of the bandgap voltage V_G is included. The temperature at the inflection point, T_{INF}, will make the partial derivative in (11) equal to zero. It is difficult to get a closed form solution of T_{INF} from (11). However, Newton-Raphson method can be applied to find the local maxima of I_1 and the corresponding T_{INF}.

Equation (11) includes several circuit parameters, such as R_0, R_1 and junction areas. Then, it can be concluded that the inflection point of the reference will move with those parameters. The relationship of the inflection point and the circuit parameters can be investigated by numerical simulation. In this work, the value of R_0 is chosen as the variable parameter. Fig. 2 illustrates the inflection point of the voltage reference against R_0. The solid line represents the result from analysis and numerical simulation. The dotted line and the star line are from Spectre simulation with 80dB and 70dB op amp gain respectively. The offset voltage of the op amp is assumed to be zero. It is also assumed that in Spectre simulation the circuit has no mismatch errors. As can be seen, three curves in Fig. 2 are in close agreement. With the lower op amp gain, the larger deviation from the analysis should be expected.

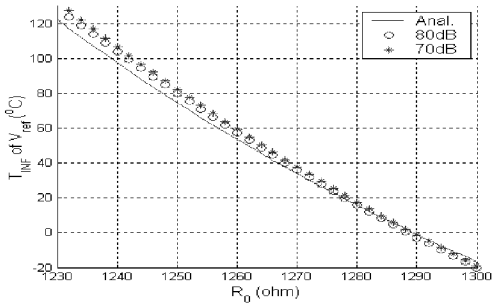

Figure 2. The inflection point of V_{ref} changing with R_0

However, the shape of the curve can still be well estimated. The slope of the curve shows good adjustability of the inflection point by changing R_0.

2) Output voltage at the inflection point

The value of the output at the inflection point can be derived. The partial derivative in (11) equals zero at the inflection points T_{INF}, then we have

$$\frac{k}{qR_1}\ln\left(\frac{k}{qR_0\sigma A_1 T_{INF}^{\,r-1}}\ln\frac{A_2}{A_1}\right)= \frac{k(r-1)}{qR_1}-\frac{k}{qR_0}\ln\frac{A_2}{A_1}+\frac{2\alpha T_{INF}}{(T_{INF}+\beta)R_1}-\frac{\alpha T_{INF}^{\,2}}{(T_{INF}+\beta)^2 R_1} \quad . \quad (12)$$

The current at the inflection point can be rewritten as

$$I_{1INF}=\left[\frac{kT_{INF}}{q}(r-1)+V_{G0}+\frac{\alpha T_{INF}^{\,2}}{T_{INF}+\beta}-\frac{\alpha T_{INF}^{\,3}}{(T_{INF}+\beta)^2}\right]\frac{1}{R_1} . \quad (13)$$

Thus, the reference voltage at T_{INF} can be expressed in

$$V_{ref}(T_{INF})=\left[\frac{kT_{INF}}{q}(r-1)+V_{G0}+\frac{\alpha T_{INF}^{\,2}}{T_{INF}+\beta}-\frac{\alpha T_{INF}^{\,3}}{(T_{INF}+\beta)^2}\right]\frac{R_3}{R_1} . \quad (14)$$

It should be noted that (14) is based on the assumption that the current mirror is an ideal unity gain current mirror. However, with the effect of channel modulation, the current through R_3 is not equal to the current I_1. The comparison of simulated and analytical V_{ref} is shown in Fig. 3. Mismatch between I_1 and I_3 introduces a voltage shift between the simulated and the analytical results. As can be seen, the reference voltage at the inflection point increases with the temperature in the given temperature range. From (14), these voltages can be easily regulated by adjusting R_3. More importantly, the change of R_3 will not affect the inflection point of the bandgap curve as shown in (12). That means the bandgap curves can be shifted up or down without changing their shapes.

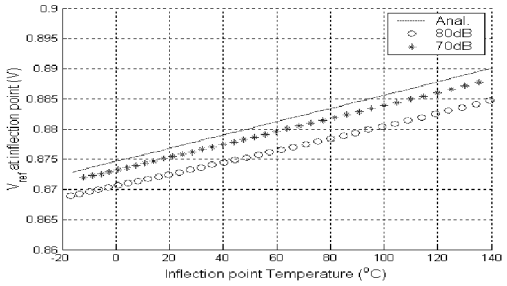

Figure 3. The reference voltage changing with temperature

3) Curvature of the linear compensated bandgap curve

The curvature of the bandgap curve shows how fast it changes with temperature near the inflection point and is directly related to its temperature coefficient. Because what the temperature coefficient indicates is the percentage change of the parameter with temperature, the normalized second order derivative at T_{INF} is calculated to evaluate its curvature as in

$$C_{INF}=\frac{1}{V_{INF}}\frac{\partial^2 V_{ref}}{\partial T^2}\Big|_{T=T_{INF}}=\frac{1}{I_{1INF}}\frac{\partial^2 I_1}{\partial T^2}\Big|_{T=T_{INF}} , \quad (15)$$

where C_{INF} is the normalized curvature at the inflection point. Substituting (11) and (13) into equation (15), this curvature can be rewritten as

$$C_{INF}=\frac{-\frac{k(r-1)}{qT_{INF}}-\frac{2\alpha\beta^2}{(T_{INF}+\beta)^3}}{\frac{kT_{INF}}{q}(r-1)+V_{G0}+\frac{\alpha T_{INF}^{\,2}}{T_{INF}+\beta}-\frac{\alpha T_{INF}^{\,3}}{(T_{INF}+\beta)^2}} . \quad (16)$$

It is noticed that there are only process parameters and temperature in (16). Therefore, the curvature at the inflection point is independent on any circuit parameter. Two different implementations of the circuit shown in Fig. 1 are simulated in Spectre. The currents through Q_1 in Circuit 1 and Circuit 2 are 20uA and 50uA respectively, and the circuit parameters, such as R_0, R_1 and the area ratio, are quite different from each other. The op amp gain is 80dB. In Fig. 4, the simulated curvatures of I_1 at different inflection point temperatures are compared to the analytical values. As shown in the figure, the simulated results are in close agreement with the analysis. The normalized curvatures of V_{ref} are also plotted. Because of the effects of non-ideal current mirror, there are considerable deviations between two circuits as well as between the simulated and analytical results. In addition, in real circuits, process variations, mismatch errors and TC of the resistors can also cause curvature change.

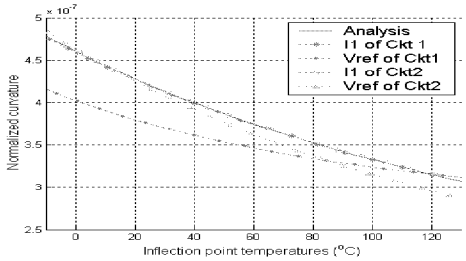

Figure 4. 2nd derivative of the inflection points against inflection point temperatures

III. Proposed Method of Designing High-precision Reference

It is well known that the bandgap circuit with linear compensation has a small TC, provided the temperature operating range is small and the inflection point is appropriately placed in the desired temperature operating region. If the inflection point is not appropriately placed, the TC will become quite large since the derivative of the output voltage with respect to temperature increases rapidly at temperatures away from the inflection point. It is apparent that quite high resolution can be achieved only if the device always operates near the inflection point. The proposed method is to use multiple references with multiple inflection points to implement a high-resolution reference by stepping from one reference output to another as temperature changes. Therefore, advantage of the local temperature stability of each reference can be taken. Fig. 5 shows Spectre simulation results of the case that the whole temperature region from T_1 to T_2 is covered by three references. With their inflection points appropriately distributed, the upper window illustrates that the achievable resolution is more than 13 bits, which is much higher than the best resolution achieved by a single curve (about 10 bits). It is clear that the achievable resolution is directly related to the number of references in use. The relationship is shown in Table 1.

The bandgap structure we have analyzed shows good features of easily adjusting its inflection point and reference voltage by choosing R_0 and R_3 respectively. It has great potentials of implementing multiple references. There are three major factors that make the design of a multi-segment voltage reference challenging. The first is the precise positioning of the inflection points so that operation near an inflection point can be attained. The second is the issue of aligning each segment with desired reference level and accuracy. The third is in establishing a method for stepping from one segment to another at precisely the right temperature in a continuous way. The modeling of the inflection point can be utilized to predict proper R_0 values for well-distributed inflection points. However, with process variations, mismatch errors and finite op amp gain, modeling errors in prediction are inevitable. Then, a local on-chip heater and a temperature sensor are incorporated to help. The method of alignment and continuous

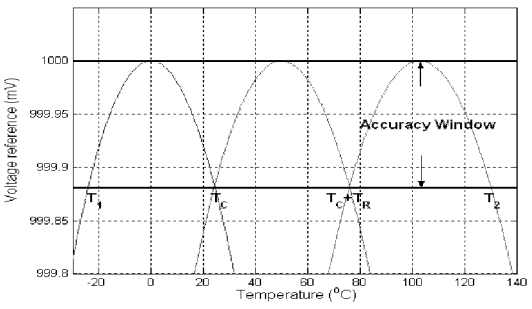

Figure 5. A three-segment voltage reference

TABLE I. TCs WITH DIFFERENT NUMBERS OF CURVES

# Curves	3	4	6	9
TC(ppm/°C)	0.8	0.4	0.2	0.1
Accuracy(Bits)	13	14	15	16

curve transfer can also be achieved as following. With a specified reference level and accuracy, the number of segments and the temperature range covered by each segment can be determined based on their curvatures. At the beginning, we start from a calibrated segment, which could be done in the production test by setting appropriate values for R_0 and R_3. When the ambient temperature rises to a temperature T_C so that the output reference is right at the boundary of the desired accuracy window, we start to find the next segment, which can provide reference with required accuracy for next T_R degrees, where T_R is the temperature region covered by the next segment at shown in Fig. 5. To find a proper value for R_0 the heater is used to intentionally change the temperature of the bandgap circuit from T_C to T_C+T_R. It is clear that only the right segment have the references at those two temperatures equal. Thus with the help of heater, the value of R_0 can be determined by comparing those two references. After the segment is found, we can align this segment with the original one at temperature T_C by comparing two references from different segments at this temperature. Then an appropriate R_3 value can be obtained. For each time the temperature sensor indicates the current temperature rises to temperature T_C a continuous transfer can be made to the next segment.

IV. Conclusion

In this work, a specific current mode bandgap structure is systematically characterized based on theoretical analysis. Three of the most important features of the circuit, the value of the bandgap output, the relationship of the inflection point and the circuit parameters, the curvature of the bandgap curve, are investigated. Those characteristics show that it has great potentials of providing high-precision references. The proposed approach is described.

References

[1] P. R. Cray and R. G. Meyer, *Analysis and Design of Analog Integrated Circuits,* 4th Ed. New York: Wiley, 2001.

[2] Y. P. Tsividis, "Accurate analysis of temperature effects in I_C-V_{BE} characteristics with application to bandgap reference sources," *IEEE J. Solid-State Circuit*, vol. SC-15, pp. 1076-1084, Dec. 1980.

[3] S. L. Lin and C. A. T. Salama, "A VBE(T) model with application to bandgap reference design," *IEEE J. Solid-State Circuits*, vol. SC-20, pp. 1283-1285, Dec. 1985.

[4] P. K. T. Mok and K. N. Leung, "Design considerations of recent advanced low-voltage low-temperature-coefficient CMOS bandgap voltage reference," *IEEE Custom Integrated Circuits Conference*, Orlando, Florida, USA, pp. 635-642, Oct. 2004.

[5] H. Banda, H. Shiga, A. Umezawa, T. Tanzawa, S.; Atsumi and K. Sakui, "A CMOS bandgap reference circuit with sub-1-V operation," IEEE J. of Solid-State Circuits, vol. 34, pp. 670-674, May 1999.